Proceedings of the 36th Chinese Control Conference
July 26-28, 2017, Dalian, China

Fault Tolerance and Overmodulation Algorithm for Three Level Neutral Point Clamped Inverters

Ming Zhang[1], Ze Li[2], Yuanbo Guo[2], Xiaohua Zhang[1, 2]

1. School of Electrical Engineering & Automation, Harbin Institute of Technology, Harbin 150001, China
E-mail: zmstc19719@126.com,

2. School of Electrical Engineering, Dalian University of Technology, Dalian 116024, China
E-mail: dlut_lize@163.com, gyb@dlut.edu.cn, xh_zhang@dlut.edu.cn

Abstract: It has been a hot issue and also a difficulty to study the fault tolerance of multilevel converters. The topology changes to eight-switch three-phase inverter (ESTPI) if one leg of three-level NPC inverter is failed. An optimal modulation algorithm of ESTPI is proposed in this paper. Due to the loss of one leg, the DC-link voltage utilization of ESTPI is reduced by half. Hence, an overmodulation algorithm based on superposition principle is proposed to improve DC-link voltage utilization, without increasing DC-link voltage. The proposed method is easier to implement compared with conventional overmodulation strategies for less computation. Theoretical proof and experimental results show that the proposed overmodulation algorithm is effective, and the DC-link voltage utilization can be increased maximally by 10.3%.

Key Words: Fault tolerance, eight-switch three-phase inverter, superposition principle, overmodulation

1 Introduction

With characteristics of low output harmonics, EMI and switching stress, three-level topologies are increasingly used in high-voltage and high-power applications, such as new energy, high speed railway and electronic converters. Compared with two-level system, the failure rate of three-level system is higher as a result of using more semiconductors. To improve system reliability and stability, it is essential to study fault tolerant control strategies of three-level inverter.

Three-level neutral-point-clamped topology is widely used, as a typical topology of multilevel inverter. Its fault tolerant topologies can be divided into two types: four-leg topology and three-leg topology [1-3]. In four-leg topology, a redundant leg is added to the inverter. In normal mode, the redundant leg is used for regulating neutral-point voltage. In fault tolerant mode, the failure leg is replaced by the redundant leg, to make sure the inverter is working normally with three healthy legs. On the other hand, the three-leg topology cuts the failure leg to avoid a secondary failure, and changes to eight-switch three-phase (ESTP) topology in fault tolerant mode (see in Fig. 1). Researches currently are mostly focused on the fault-tolerant topologies of three-level inverter, yet its fault-tolerant control strategies need further study.

A lot of attentions on the control strategies of ESTPI have been made recent years. The SVPWM based control strategies are proposed in [4] and [5], ensuring the output voltages sinusoidal and symmetrical after fault. Other methods based on CBPWM are presented in [6] and [7]. In [6], the phase difference between modulation functions is changed from 2π/3 to π/3 to obtain symmetrical output voltages. However, the two methods discussed above are proved to be equivalent for using a same modulation function in [7]. Besides, the switchover process from normal mode to fault tolerant mode is analyzed in [8] and [9], so that a quick and smooth dynamic process is implemented. From the methods discussed above, there are two problems still need to be solved. 1) The methods realized that inverter is able to keep working after fault, but the DC-link voltage utilization drops to half. 2) The merits and drawbacks of these methods should be compared and summarized.

Considering the above problems, the typical fault tolerant control strategies in literatures are discussed in this paper. An optimal one is concluded with best control performance and lowest computation. An overmodulation strategy based on superposition principle of ESTPI is proposed to increase the DC-link voltage utilization after fault.

2 Fault-Tolerant Control Strategy of Three-Level NPC Inverter

2.1 Eight-Switch Three-Phase Inverter

Fig. 1(b) shows the eight-switch three-phase topology after isolating the faulty leg (taking phase *a* as an example). Assuming that U_{dc} is constant, $C_1 = C_2$, the pole voltage u_{xO} and the switching functions S_x of two normal legs can be described in Table 1 ($x = b, c$).

Table 1: Pole voltages and switching functions of ESTPI

S_{x1}	S_{x2}	S_{x3}	S_{x4}	S_x	u_{xO}
on	on	off	off	1(P)	$U_{dc}/2$
off	on	on	off	0(O)	0
off	off	on	on	-1(N)	$-U_{dc}/2$

The voltage vector $\boldsymbol{U}_r$ in two-phase stationary coordinate, namely the $\alpha\beta$-plane can be obtained by the following expression

$$\boldsymbol{U}_r = \frac{2}{3}\left(u_{aO}e^{j0} + u_{bO}e^{j\frac{2\pi}{3}} + u_{cO}e^{j\frac{4\pi}{3}} \right) \quad (1)$$

*This work is supported by National Nature Science Foundation of China (51407023, 51377013), China Postdoctoral Science Foundation (2013M540224)

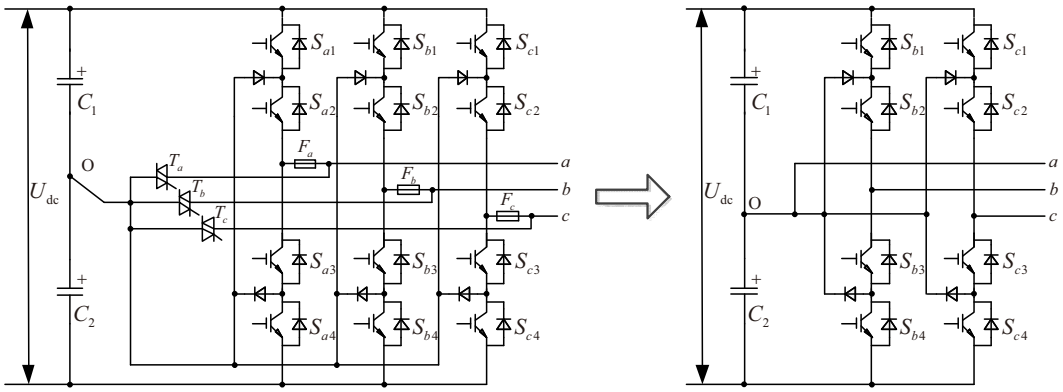

Fig. 1: Eight-switch three-phase inverter (ESTPI)

Connected to the neutral-point of capacitors, phase *a* can only output zero level. So the number of basic voltage vectors decreases from 27 to 9 after fault, including 6 small-vectors, 2 medium-vectors and 1 zero-vector. The voltage vector distribution of ESTPI is shown in Fig. 2. The region of voltage vectors is reduced to the inner diamond, and the linear modulation region turns into the inscribe circle of the inner hexagon. Hence, the DC-link voltage utilization decreases to half, and the max amplitude of the output line voltage is $U_{dc}/2$.

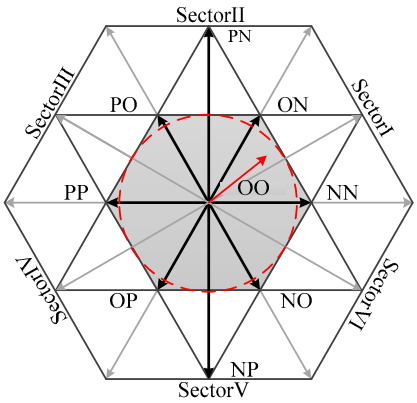

Fig. 2: Voltage vector distribution of ESTPI

2.2 Analysis and Comparison of Fault-Tolerant Control Strategies of ESTPI

The fault tolerant control strategies can be divided into two types based on the modulation methods they use: SVPWM and CBPWM. The methods based on SVPWM and CBPWM turn out to be equivalent in [7], since they get a same modulation function. Therefore, only the methods based on SVPWM are discussed in this paper.

According to the different voltage vectors they used, there are three fault-tolerant control strategies of ESTPI (see in Fig. 3).

1. SVPWM-I

As shown in Fig. 3(a), all the 9 voltage vectors are used to synthesize the reference vector. The modulation region is divided into 8 sectors. Two small-vectors adjacent to the sector and the zero-vector are used as basic voltage vectors in Sector I, IV, V and VIII. One medium-vector, one small-vector and the zero-vector are used in the rest sectors. Compared with the conventional 7-segment SVPWM, only 5-segment SVPWM can be used here without the redundant small-vectors. Table 2 shows the vector sequence in each sector.

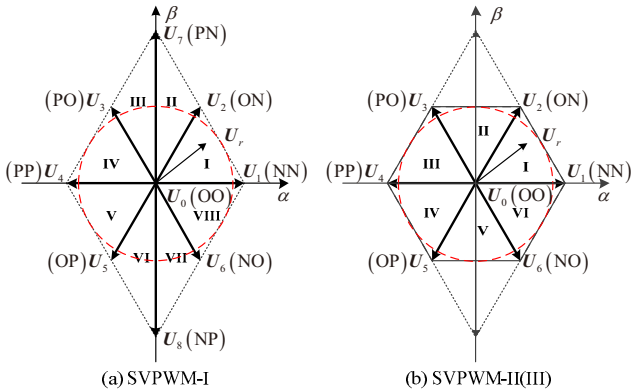

Fig. 3: Different control strategies of ESTPI

Table 2: Vector sequence by SVPWM-I

Sector	Vector Sequence
I	OO→ON→NN→ON→OO
II	OO→ON→PN→ON→OO
III	OO→PO→PN→PO→OO
IV	OO→PO→PP→PO→OO
V	OO→OP→PP→OP→OO
VI	OO→OP→NP→OP→OO
VII	OO→NO→NP→NO→OO
VIII	OO→NO→NN→NO→OO

Researches show that the use of medium-vector in three-level inverter will lead to uncontrollable fluctuation of neutral-point potential. Furthermore, the output voltages come out to be unbalanced modulated by SVPWM-I, when the amplitude of reference line voltage is greater than $U_{dc}/2$, namely in overmodulation region. Therefore, the application of SVPWM-I is limited.

2. SVPWM-II

Only small-vectors and zero-vector are used to synthesize the reference vector. There are 6 sectors in the modulation region. The vector sequence is shown in Table 3.

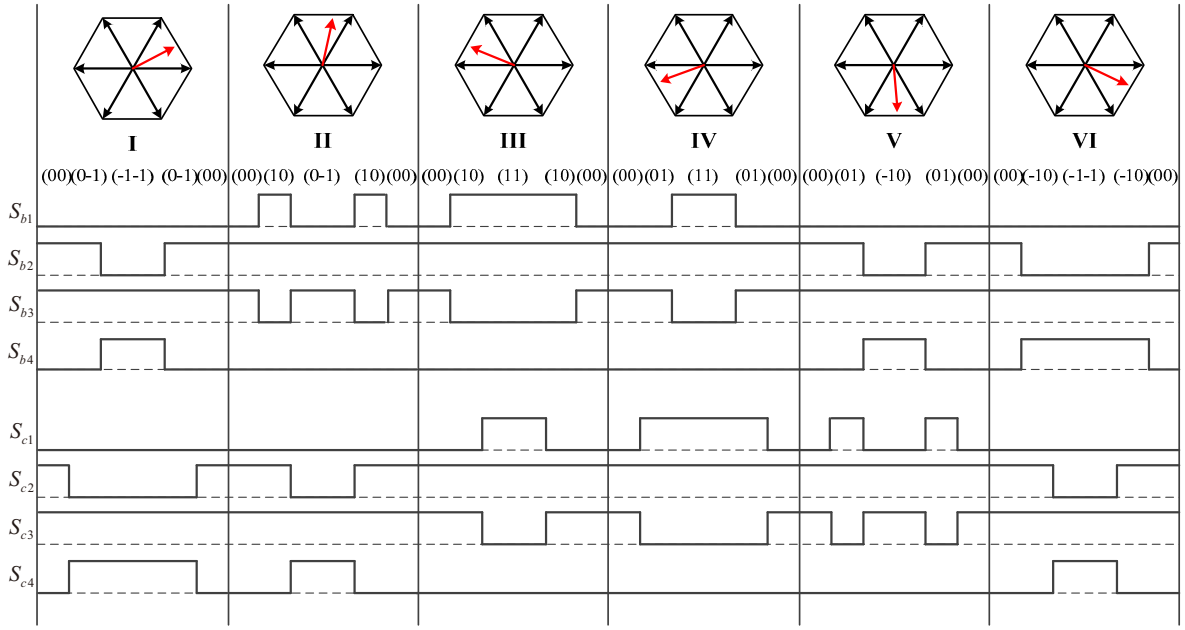

Fig. 4: Sequencing of power switches in each sector by SVPWM-II

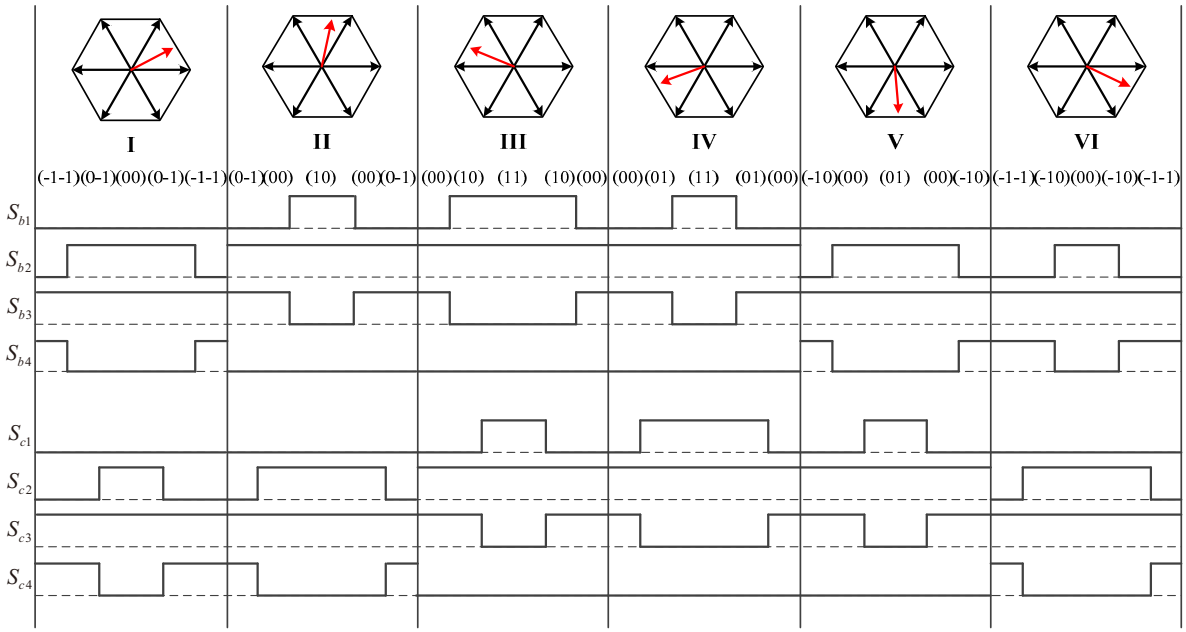

Fig. 5: Sequencing of power switches in each sector by SVPWM-III

Table 3: Vector sequence by SVPWM-II

Sector	Vector Sequence
I	OO→ON→NN→ON→OO
II	OO→PO→ON→PO→OO
III	OO→PO→PP→PO→OO
IV	OO→OP→PP→OP→OO
V	OO→OP→NO→OP→OO
VI	OO→NO→NN→NO→OO

The sequencing of power switches in each sector is shown in Fig. 4. Starting with zero-vector, the sequencing has a smooth transition between two contiguous periods. However, the switch state changes four times during the switching period in sector II and V, increasing switching loss and making drive pulse more complicate.

3. SVPWM-III

The same as SVPWM-II, SVPWM-III also uses small-vectors and zero-vector. But the synthesizing vector sequence is changed to improve the performance in sector II and V, as shown in Table 4

Table 4: Vector sequence by SVPWM-III

Sector	Vector Sequence
I	NN→ON→OO→ON→NN
II	ON→OO→PO→OO→ON
III	OO→PO→PP→PO→OO
IV	OO→OP→PP→OP→OO
V	NO→OO→OP→OO→NO
VI	NN→NO→OO→NO→NN

To guarantee that switch states change two times in every switching period, the synthesizing vector sequence no longer starts with zero-vector (see in Fig. 5). However, extra switching states appear when sector changes. Compared with two methods above, SVPWM-III obtains lower switching loss and computation.

3 Overmodulation strategy of ESTPI Based on Superposition Principle

From previous analysis, the max amplitude of output line voltage is reduced by half after fault. Thus, the system performance will be seriously affected in certain occasions, like grid-connected system and motor servo system. The overmodulation strategy is the only way to increase DC-link voltage utilization without increasing DC-link voltage.

3.1 Description of Superposition Principle

The modulation index m of ESTPI is defined as

$$m = \frac{\pi \cdot U_{\mathrm{r}}}{U_{\mathrm{dc}}} \tag{2}$$

Based on the value of modulation index m, there are three operation modes, namely linear mode $(0 \le m < 0.907)$, overmodulation mode I $(0.907 \le m < 0.952)$, and over-modulation mode II $(0.952 \le m < 1)$. In linear mode, the modulation method is just the same as SVPWM-III analyzed above. Only the overmodulation modes are discussed here.

1. Overmodulation mode I $(0.907 \le m < 0.952)$

The overmodulation coefficient K_1 in this mode can be defined as follows

$$K_1 = \frac{m - 0.907}{0.952 - 0.907} \quad (0 \le K_1 < 1) \tag{3}$$

According to superposition principle, the reconfigured reference vector is given as

$$\boldsymbol{U}_{\mathrm{r}} = (1 - K_1) \cdot \boldsymbol{U}_{\mathrm{sin}} + K_1 \cdot \boldsymbol{U}_{\mathrm{hex}} \tag{4}$$

where $\boldsymbol{U}_{\mathrm{sin}}$ is the vector whose end-point trajectory is the inscribe circle of the inner hexagon, and $\boldsymbol{U}_{\mathrm{hex}}$ is the vector whose end-point trajectory is the inner hexagon. Their expressions are given as (taking sector I as an example).

$$\begin{cases} \boldsymbol{U}_{\mathrm{sin}} = \sqrt{3} U_{\mathrm{dc}} e^{j\theta} / 6 \\ \boldsymbol{U}_{\mathrm{hex}} = \left(\sqrt{3} U_{\mathrm{dc}} e^{j\theta} / 6 \right) \cos(\pi/6 - \theta) \end{cases} \tag{5}$$

2. Overmodulation mode II $(0.952 \le m < 1)$

Similarly, the overmodulation coefficient K_2 in this mode is defined as

$$K_2 = \frac{m - 0.952}{1 - 0.952} \quad (0 \le K_2 < 1) \tag{6}$$

The reconfigured reference vector is given as

$$\boldsymbol{U}_{\mathrm{r}} = (1 - K_2) \cdot \boldsymbol{U}_{\mathrm{hex}} + K_2 \cdot \boldsymbol{U}_{\mathrm{six}} \tag{7}$$

where $\boldsymbol{U}_{\mathrm{hex}}$ is the same vector as described in over-modulation mode I; $\boldsymbol{U}_{\mathrm{six}}$ is one of the six small-vectors, and can be described by the following expression (taking sector I as an example).

$$\boldsymbol{U}_{\mathrm{six}} = \begin{cases} U_{\mathrm{dc}} e^{\mathrm{j}0} / 3 & (0 \le \theta < \pi/6) \\ U_{\mathrm{dc}} e^{\mathrm{j}\pi/3} / 3 & (\pi/6 \le \theta < \pi/3) \end{cases} \tag{8}$$

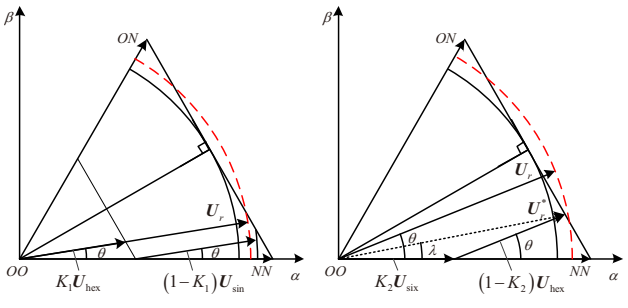

(a) Overmodulation Mode I (b) Overmodulation Mode II

Fig. 6: Diagram of reconfigured reference vector according to superposition principle

3.2 Proof of Superposition Principle

Assuming that the output phase voltage is balanced, its expression is described as

$$\begin{cases} u_{an} = \sum_{n=1}^{\infty} A_n \sin(n\omega_0 t + \alpha_0) \\ u_{bn} = \sum_{n=1}^{\infty} A_n \sin(n\omega_0 t + \alpha_0 - 2\pi/3) \\ u_{cn} = \sum_{n=1}^{\infty} A_n \sin(n\omega_0 t + \alpha_0 - 4\pi/3) \end{cases} \tag{9}$$

where A_n is the amplitude of the nth harmonic. ω_0 is the fundamental angular frequency, and α_0 is the initial phase.

The reference vector is calculated as

$$\begin{aligned} \boldsymbol{U}_{\mathrm{r}} &= \frac{2}{3}\left(u_{an} e^{\mathrm{j}0} + u_{bn} e^{\mathrm{j}\frac{2\pi}{3}} + u_{cn} e^{\mathrm{j}\frac{4\pi}{3}} \right) \\ &= \sum_{n=1}^{\infty} A_n \left(\sin(n\omega_0 t + \alpha_0) - \mathrm{j}\cos(n\omega_0 t + \alpha_0) \right) \end{aligned} \tag{10}$$

From (9) and (10), it can be concluded that the phase a voltage can be obtained by projecting the reference voltage vector onto the α-axis.

In overmodulation mode I, the projection of the reconfigured reference vector on the α-axis is calculated as follows by (3)-(5) (taking sector I as an example).

$$U_{\mathrm{r}\alpha}(\theta) = \mathrm{Re}(\boldsymbol{U}_{\mathrm{r}}) = \frac{\sqrt{3} U_{\mathrm{dc}}}{6} \left[(1 - K_1) + \frac{K_1}{\cos(\pi/6 - \theta)} \right] \cdot \cos\theta \tag{11}$$

$U_{\mathrm{r}\alpha}(\theta)$ in other sectors can be derived in the same way. Then the complete expression of phase a voltage in a fundamental cycle is obtained. By Fourier transformation of $U_{\mathrm{r}\alpha}(\theta)$, the fundamental voltage amplitude is calculated as

$$a_1 = \frac{1}{\pi} \int_0^{2\pi} U_{\mathrm{r}\alpha}(\theta) \cos\theta \, \mathrm{d}\theta \tag{12}$$

Substituting (3) and (11) into (12), the amplitude of fundamental voltage can be simplified as

$$a_1 = \frac{U_{\mathrm{dc}}}{\pi} (0.9905m + 0.0083) \quad (0.907 \le m < 0.952) \tag{13}$$

Similarly, phase a voltage in overmodulation mode II can be deduced according to superposition principle as

$$U_{\mathrm{r}\alpha}(\theta) = \begin{cases} \frac{\sqrt{3} U_{\mathrm{dc}}}{6} \cdot \frac{(1 - K_2)}{\cos(\pi/6 - \theta)} \cdot \cos\theta + \frac{U_{\mathrm{dc}}}{3} \cdot K_2 & (0 \le \theta < \pi/6) \\ \frac{\sqrt{3} U_{\mathrm{dc}}}{6} \cdot \frac{(1 - K_2)}{\cos(\pi/6 - \theta)} \cdot \cos\theta + \frac{U_{\mathrm{dc}}}{6} \cdot K_2 & (\pi/6 \le \theta < \pi/3) \end{cases} \tag{14}$$

According to (6), (14) and (12), the amplitude of fundamental voltage is simplified as:

$$a_1' = \frac{U_{dc}}{\pi}(1.0104m - 0.0104) \quad (0.952 \le m < 1) \qquad (15)$$

As defined in (2), the ideal amplitude of output phase voltage is $U_r = mU_{dc}/\pi$. Fig. 7 shows the amplitude of output phase voltage in function of m, comparing the ideal amplitude with the one obtained by the proposed method. Results show that the proposed method can implement the overmodulation of ESTPI, and the amplitude of output phase voltage is equal to the given value correctly.

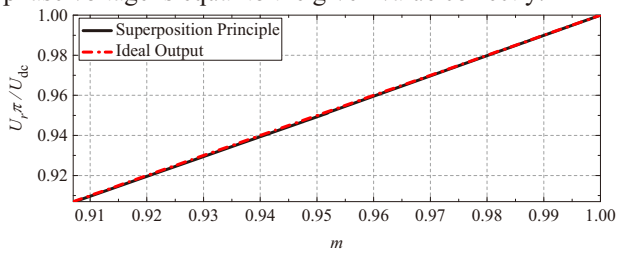

Fig. 7: Amplitude of output phase voltage in function of m

4 Experimental Results

The experiment platform of ESTPI controlled by dSPACE is built to validate the feasibility of the proposed strategy (see in Fig. 8). The DC-link voltage and capacitance are set as 500V and 3600μF respectively, and the switching frequency is 1000 Hz. The parameters of induction motor are chosen as: P = 2200W, R_s = 2.31Ω, R_r = 1.938Ω, L_s = 0.2862H, L_r = 0.2862H, L_m = 0.2839H and p = 2.

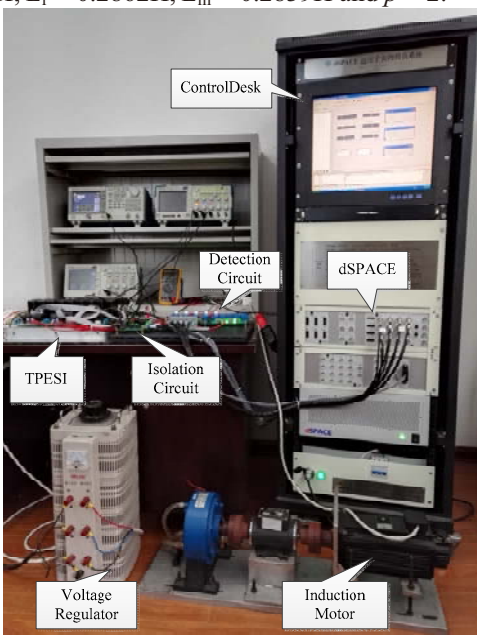

Fig. 8: Experiment platform of ESTPI

The modulation index is set to 0.7, 0.93 and 0.98 in three modulation mode, respectively. Then the waveforms and spectrograms of output line voltage are shown in Fig. 9, Fig. 10 and Fig. 11.

The theoretical amplitude of output line voltage can be given as:

$$U_{line} = \sqrt{3}\, mU_{dc}/\pi \qquad (16)$$

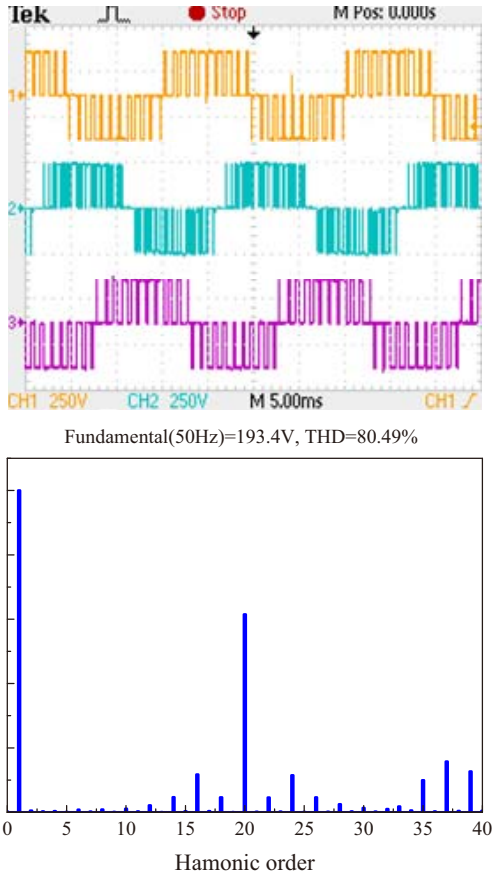

Fig. 9 Waveform and spectrogram of output line voltage in linear mode (m=0.7)

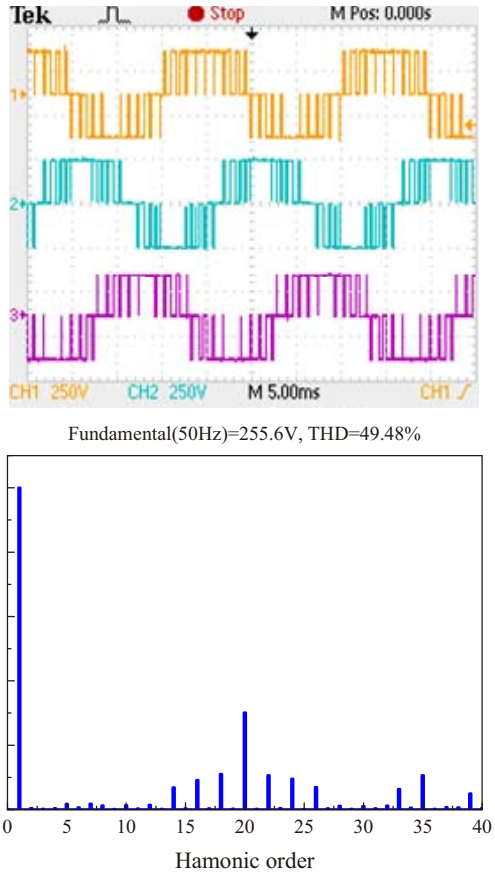

Fig. 10 Waveform and spectrogram of output line voltage in overmodulation mode I (m=0.93)

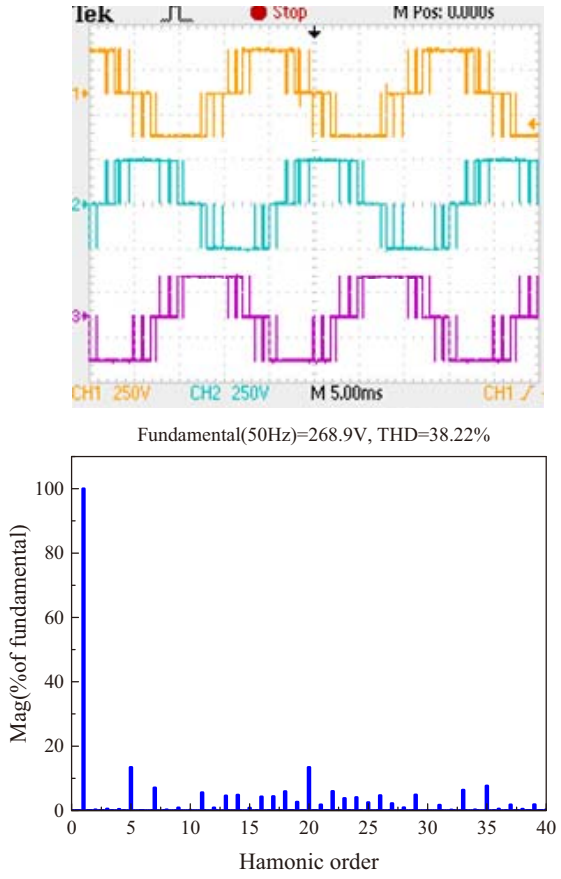

Fig. 11 Waveform and spectrogram of output line voltage in overmodulation mode II (m=0.98)

The figures above show that the output voltages are still balanced after fault, and the actual value obtained by the experiments is equivalent to that calculated by (16). Besides, the max amplitude of output line voltage reaches 275.7V, 10.3% higher than that without overmodulation strategy. That means the proposed strategy is correct and effective.

5 Conclusion

Several fault tolerant control strategies for ESTPI are compared in this paper, and the one with optimal performance is concluded. Moreover, an overmodulation method based on superposition principle is proposed to increase DC-link voltage utilization of ESTPI. The effectiveness of the proposed method is demonstrated not only by theoretical proof, but also by experimental results. The proposed overmodulation method will increase the DC-link voltage utilization by 10.3%.

References

[1] Lezana P, Pou J, Meynard T A, et al, Survey on fault operation on multilevel inverters, *IEEE Transactions on Industrial Electronics*, 57(7): 2207-2218, 2010.

[2] Zhang W, Xu D, Enjeti P N, et al, Survey on fault-tolerant techniques for power electronic converters, *IEEE Transactions on Power Electronics*, 29(12): 6319-6331, 2014.

[3] Mirafzal B, Survey of fault-tolerance techniques for three-phase voltage source inverters, *IEEE Transactions on Industrial Electronics*, 61(10): 5192-5202, 2014.

[4] Park G T, Kim T J, Kang D W, et al, Control method of NPC inverter for continuous operation under one phase fault condition, *Industry Applications Conference, 2004. 39th IAS Annual Meeting. Conference Record of the 2004 IEEE*, 2004, 4: 2188-2193.

[5] Lin B R, Wei T C, Space vector modulation strategy for an eight-switch three-phase NPC converter, *IEEE Transactions on Aerospace and electronic systems*, 40(2): 553-566, 2004.

[6] Baptista B R O, Abadi M B, Mendes A M S, et al, The performance of a three-phase induction motor fed by a three-level NPC converter with fault tolerant control strategies, *9th IEEE International Symposium on Diagnostics for Electric Machines, Power Electronics and Drives (SDEMPED),* 2013: 497-504.

[7] Liu Y, Ge X, Feng X, Two Types of Equivalent PWM Algorithms in the Full Modulation Region for Eight-switch Three-phase Inverter Based on the Superposition Principle, *Transactions of China Electrotechnical Society*, 30(15): 96-108, 2015.

[8] Abdelghani H B, Abdelghani A B B, Slama-Belkhodja I, Three level fault tolerant DTC control for induction machine drives, *9th International Multi-Conference on Systems, Signals and Devices (SSD)*, 2012: 1-6.

[9] Ceballos S, Pou J, Robles E, et al, Performance evaluation of fault-tolerant neutral-point-clamped converters, *IEEE Transactions on Industrial Electronics*, 57(8): 2709-2718, 2010.